Effects of the Doping ZnO on the property of Magnetic Solid Acid SO_4^{2-}/ZrO_2-Fe_3O_4

[1, 2]MEIQING FAN, [1, 2]BO REN, [1]JUN WANG* AND [1, 3]XIAOYAN JING
[1]*College of Material Science and Chemical Engineering*, *Harbin Engineering University*, *Harbin 150001*, *P.R. China.*
[2]*Department of Applied Chemistry Engineering*, *Jilin Vocational College of Industry and Technology Jilin*, *132013*, *P.R. China.*
[3]*The Key Laboratory of Superlight Materials and Surface Technology*, *Ministry of Education*, *Harbin 150001*, *PR China.*
zhqw1888@sohu.com*

(Received on 5th June 2012, accepted in revised form 9th October 2012)

Summary: Two kinds of magnetic solid acid catalysts are prepared via a simple chemical co-precipitation approach. The obtained materials are characterized by X-ray Diffraction, FT-IR Spectrometer, Different Scanning Calorimetry, Vibrating Sample Magnetometer, Transmission Electron Microscopy, High-resolution Transmission Electron Microscopy and Hammett indicator. The results indicate that the doping of ZnO restrains the phase transformation from tetragonal zirconia to monoclinic zirconia. Furthermore, the samples show a magnetic behavior. Saturation magnetization of the sample SO_4^{2-}/ZrO_2-Fe_3O_4 is smaller than SO_4^{2-}/ZrO_2-Fe_3O_4-ZnO; Transmission Electron Microscopy results indicate that the increasing ZnO makes the grains size considerably smaller, and the High-resolution Transmission Electron Microscopy shows that the doping of ZnO maintains the desired tetragonal zirconia phase, and the interplanar spacing is d(101)=0.29 nm. Hammett indicator results show that the acid strength becomes stronger because of the doping of ZnO. The synthesis of methyl laurate as the probe reactions of magnetic solid acids is studied, and the result indicates that the doping of ZnO delays the deactivation rate of catalysts.

Key words: Chemical co-precipitation; Magnetic solid acid; Nanocomposite; ZnO.

Introduction

The organic synthesis can be catalyzed by mineral acids (such as HF, H_2SO_4, or H_3PO_4) [1-3] or solid acids [4-8]. But the liquid acids are considered to be corrosive and difficult to recover from a reaction mixture. While for solid acids, the pure zirconia's super-acidic strength is more than 10 000 times higher than pure H_2SO_4 [9], so it is widely used in organic synthesis [10-12]. However, after the reaction it is desirable to separate and recover the solid acids. Therefore, a magnetic solid acid catalyst appeared. The conventional solid acid catalysts are generally separated from the liquid phase by centrifugation or filtration. Magnetic solid acid catalysts can be simply separated from the reaction products by a magnet, making the separation of solid catalysts easier and more economic. However, in higher temperature, tetragonal phase zirconia could not be possessed. In order to increase the thermal stability and acidity, a number of attempts have been made to improve the acidity of zirconia-based catalysts by incorporating different metals oxide [13-17]. But the doping of ZnO in magnetic solid acid is rarely reported.

In this study, two types of magnetic solid acid, pure zirconia with magnetic substrate (SZF) and pure zirconia with magnetic substrate and ZnO (SZFZ), are prepared.

Results and Discussion

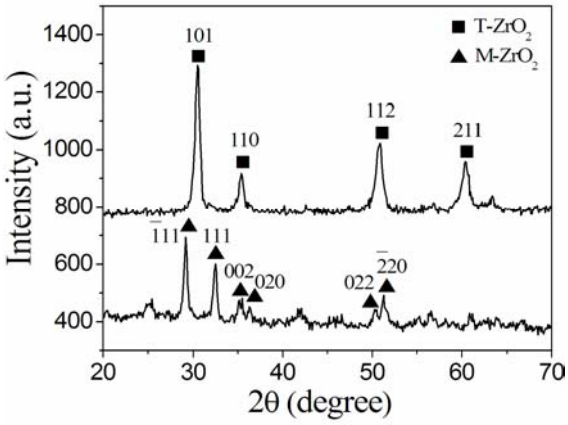

Fig. 1: XRD patterns of different samples. ((a) SZF-600; (b) SZFZ-600).

Fig. 1 shows XRD patterns of the samples calcined at 600 °C. As shown in Fig. 1(a), several peaks at 2θ = 28.19° and 2θ = 31.48° are observed,

*To whom all correspondence should be addressed.

which are indexed as ($\bar{1}$11) and (111) diffraction peaks. These are ascribed to monoclinic phase (M-ZrO_2) (JCPDS (Joint Committee on Powder Diffraction Standards) NO 24-1165). While for sample (b), the monoclinic peaks are disappeared because of ZnO additives. Moreover, the addition of ZnO stabilizes the metastable tetragonal phase (T-ZrO_2) (JCPDS NO 79-1770). A stronger peak at 2θ = 30.24° is observed, which corresponds to the (101) line. The results reveal that the introduction of ZnO improves significantly the thermal stability of the solid acid, and hinders markedly the phase transformation from tetragonal zirconia to monoclinic zirconia. The characteristics diffractions of ZnO and Fe_3O_4 can't be observed demonstrating the homogeneous distribution of amorphous ZnO and Fe_3O_4 throughout the matrix of ZrO_2.

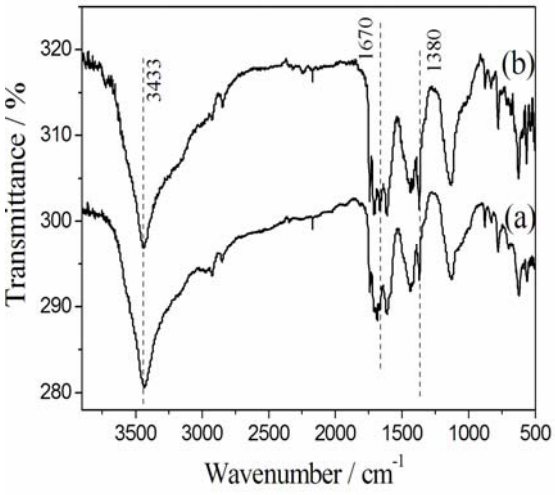

Fig. 2: IR patterns of different samples.
((a) SZF-600; (b) SZFZ-600)

The IR spectras of SZF-600 and SZFZ-600 are shown in Fig. 2. The bands at about 3433 cm^{-1} and 1670 cm^{-1} are observed, which are attributed to O-H bonds. These bonds can be attributed to the adsorption of water molecules from the air onto the surface of the catalyst [18]. The band at 1736 cm^{-1} belongs to the stretching vibration of the C=O of CO_2. This is attributed to that CO_2 molecules in air are adsorbed on the surface of the catalyst [19]. A strong band assigned to the stretching vibration of S=O is observed at 1380–1370 cm^{-1}, the surface sulfur complexes formed by the interaction of oxides with sulfate ions are highly active catalysts. The peak at 600 cm^{-1} is attributed to O-Zr band and the vibration peak of Fe-O band is at 559 cm^{-1}.

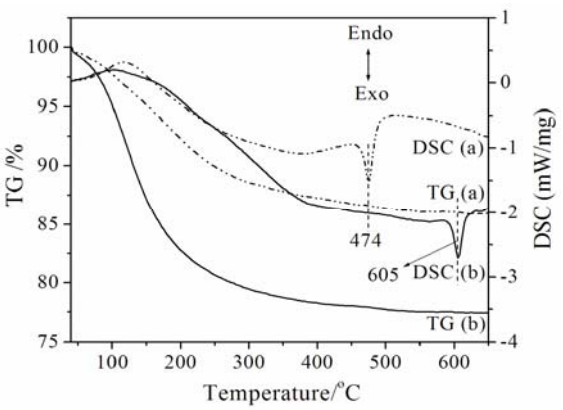

Fig. 3: TG-DSC patterns of the precursors of different samples.
((a) SZF; (b) SZFZ)

Representative results of the thermal analysis for the composite precursor powders are shown in Fig. 3. Fig. 3 shows that there is obvious mass loss from 100 to 300 °C, which is due to the release of crystal water and water adsorbed on the surface of the sample [20]. The DSC curve (sample (a)) shows that there is a weak exothermic peak without obvious mass loss at around 474 °C. This is ascribed to the transformation of zirconia from tetragonal phase zirconia to monoclinic phase zirconia. After the doping of ZnO (sample (b)), the DSC curve indicates that the transformation temperature of zirconia from tetragonal phase zirconia to monoclinic phase zirconia occurred at around 605 °C. The results indicate that transformation temperature is postponed because of the adding of ZnO, which is consistent with the XRD results.

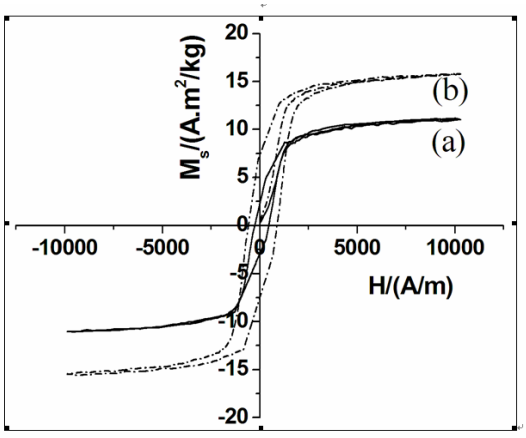

Fig. 4: VSM spectra of samples at room temperature
((a) SZF-600; (b) SZFZ-600)

The results of the VSM measurements of samples are depicted in Fig. 4. The magnetization is saturated when the field is up to 10000 A/m. The samples show a superparamagnetic behavior. Saturation magnetization of the sample (b) is 16 $A \cdot m^2/kg$, which is stronger than that of sample (a) (10 $A \cdot m^2/kg$) . The reason for the difference between (a) and (b) is that the grain sizes are decreased with the adding of ZnO. The particle size has been reported to influence the magnetic properties of materials [21, 22].

Representative TEM and HRTEM images of the SZF and SZFZ calcined at 600 °C are shown in Fig. 5 and Fig. 6, respectively. In Fig. 5, the micrograph at low magnification shows uniform lamellar crystals of about 50 nm in diameter. The HRTEM image and the corresponding Fourier filtered transformed (FFT) image can be consistently indexed using the structural data of crystals (see Fig. 5). Increasing ZnO (Fig. 6) makes the grains size considerably smaller, down to 30 nm. The results indicate that the doping ZnO inhibits the grain growth of zirconia, increases the specific surface area and improves the acidity of the catalyst.[23] The HRTEM observation indicates that the lattice spacing of SZFZ is clearly observed and supported in the laminated matrix with interphase spacings of d (101) = 0.293nm, which is agreement with XRD. The observation therefore indicates that the doping of ZnO into SZF maintains the desired tetragonal zirconia phase [24].

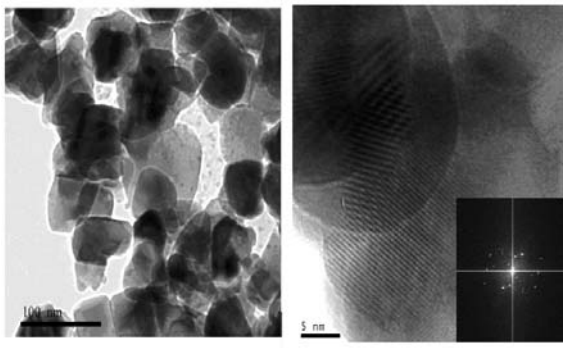

Fig. 5: TEM and HRTEM of sample SZF calcined at 600°C.

Table-1: Acid strengths of solid acid catalysts.

Catalysts	$H_o = -11.4$	$H_o = -12.0$	$H_o = -12.7$	$H_o = -13.8$
SZF-600	+	±	–	–
SZFZ-600	+	+	+	+

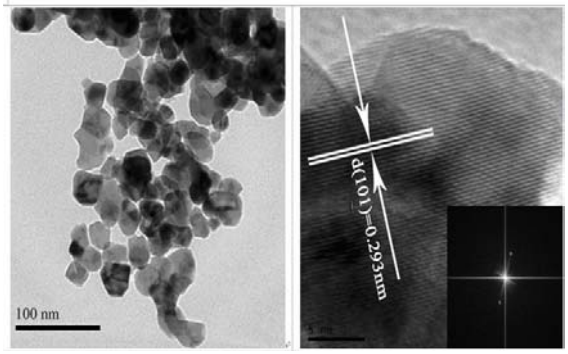

Fig. 6: TEM and HRTEM of SZFZ calcined at 600°C.

The acid strength of the catalysts was examined using a Hammett indicator dissolved in dried benzene (Table 1). From the list of results in Table 1, the sample SZF-600 is estimated to have $H_o < -11.4$, while the sample SZFZ-600 is estimated to have $H_o < -13.8$. An acid stronger than $H_o = -12$, corresponding to an acid strength of 100 % H_2SO_4, is known as a superacid. This property is attributed to the double bond nature of S=O in the complex formed by the interaction of the composite oxide ZrO_2-Fe_3O_4-ZnO with sulfate ions. In other words, the acid strength becomes stronger because of the doping of ZnO [25].

Table-2: Durabilities of catalysts (SZF and SZFZ).

Use		1st	2nd	3rd	4th	5th	6th
Conv./%	SZF	78.63	76.81	70.77	62.75	55.34	—
	SZFZ	85.35	85.35	83.95	83.46	82.19	82.17

n(lauric acid):n(methanol)=1:10; catalyst: 4 g; 80°C, 8h.

It is well known that the nature of catalysts, especially the surface properties, is one of the most important factors affecting activities of catalysts. In this research, the synthesis of methyl laurate as the probe reactions of magnetic solid acids was tested. The durabilities of catalysts were studied by repeating the experiment. As depicted in Table 2. For catalyst SZF, the activity decreases quickly after five reactions, and the percent conversion drops down from 78.63% to 55.34%. For catalyst SZFZ, the activity is kept constantly at the first two times. After the third reaction, the activity of catalyst decreases slowly, and the percent conversion drops down from 83.95% to 82.17%. It is due to the fact that the doping of ZnO delays the deactivation rate of catalysts.

Experimental

Preparation of the Solid Acid Catalysts

The uniform and highly dispersed super-paramagnetic Fe_3O_4 nanoparticles are prepared by a standard chemical co-precipitation method, as described by Gass *et al* [26] and Bruce *et al* [27]. To the mixed solution of zirconium oxychloride (32.2 g $ZrOCl_2 \cdot 8H_2O$), $Zn(CH_3COO)_2 \cdot 2H_2O$ (21.5 g), and Fe_3O_4 (0.29 g), aqueous ammonia is added dropwise with vigorous stirring until the pH is 9-10 at 45 °C. The obtained mixed solution is washed with deionized water with the assistance of an external magnetic field until the filtrate is neutral. The absence of chlorine ion is confirmed by $AgNO_3$ tests. Subsequently the solid is dipped in a $1mol \cdot L^{-1}$ $(NH_4)_2SO_4$ aqueous solution for 24 h. After filtration and drying in an oven, the solid materials are calcined for 6 h at 600 °C. The nanocomposition is designated as SZFZ-600. SZF-600 was synthesized under similar experimental conditions without the addition of ZnO.

Characterization

Powder X-ray diffraction (XRD) patterns are recorded on a Rigaku D/max-IIIB diffractometer using Cu Kα radiation (λ=1.5406 Å). IR spectra on KBr pellets of the samples are recorded on a Nicolet FT-IR spectrometer. Different scanning calorimetry (DSC) of the as-synthesized sample (10 mg) is performed on a NEZSCH STA 409PC thermoanalyzer. The analysis is carried out in Ar atmosphere in the temperature range 400-800°C with a heating rate of 10 °C/min. Magnetic hysteresis loops are measured using a vibrating sample magnetometer (VSM, JDAW–2000). Transmission electron microscopy (TEM) and high-resolution transmission electron microscopy (HRTEM) experiments are carried out on a PHILIPS CM 200 FEG electron microscope with an acceleration voltage of 200 kV. Samples dispersed in ethanol are spread on holey amorphous carbon film deposited on copper grids. The surface acidity and acid strength of the catalysts were determined by titration with n-butylamine using the Hammett indicators. The titration was carried out by dispersing 0.05 g of catalyst in 5mL of dry benzene; two indicator drops in benzene solution were then added to the resulting dispersed solution and the titration was done with a solution of n-butylamine (0.01N). The acidity was calculated in mole of acid sites per gram of catalyst and the acidity strength was expressed in terms of the Hammett acidity (H_0)[28].

Conclusion

(1) The XRD study shows that the doping of ZnO restrains the phase transformation from tetragonal zirconia to monoclinic zirconia; (2) The samples show a magnetic behavior. Saturation magnetization of the sample SZF is smaller than SZFZ;(3) TEM results indicate that the doping ZnO inhibits the grain growth of zirconia, increases the specific surface area and improves the acidity of the catalyst. The HRTEM shows that the doping of ZnO into SZF maintains the desired tetragonal zirconia phase, and the interplanar spacing is d(101)=0.29 nm;(4) Hammett indicator results show that the acid strength becomes stronger because of the doping of ZnO;(5) The doping of ZnO delays the deactivation rate of catalysts.

Acknowledgement

This work was supported by the Fundamental Research Funds of the Central University, Science and Technology Planning Project from Education Department of Heilongjiang Province (11553044), High Education Doctoral Fund (160100110010), Special Innovation Talents of Harbin Science and Technology (2010RFXXG007), the foundation of Harbin Engineering University (No. HEUFT07053), Technology Planning Project from Education Department of Jinlin Province (No. [2012] 468 and No. [2012] 467).

References

1. P. M. Esteves, C. L. Araújo, B. A. C. Horta, L. J. Alvarez and C. M. Zicovich Wilson. *The Journal of Physical Chemistry* B, **109**, 12946 (2005).
2. D. W. F. Brilman, N. G. Meesters, W. P. M. S.Van and G. F Versteeg, *Catalysis Today*, **317**, 66 (2001).
3. M. Freccero and R. Gandolfi, *Journal of Organic Chemistry*, **70**, 7098 (2005).
4. Y. Ikeda, M. Asadullah and K. Fujimoto, *The Journal of Physical Chemistry* B, **105**, 10653 (2001).
5. K. Gong, S. Chafin, K. Pennybaker, D. Fahey and B. Subramaniam, *Industrial and*

Engineering Chemistry Research, **47**, 9072 (2008).
6. N. S.Langeroodi, *Journal of the Chemical Society of Pakistan*, 32, 125 (2010).
7. Q. Zhang and R. M. Mohring, *Industrial and Engineering Chemistry Research*, **48**, 1603 (2009).
8. X. Fu, Z. Dai, S. Tian, J. Long, S. Hou and X. Wang, *Energy Fuels*, **22**, 1923 (2008).
9. Y. X. Li, D. Zhang, L. Sun, M. Xu, W. G. Zhou and X. H.Liang, *Applied Energy*, **2369**, 87 (2010).
10. I. V. Kozhevnikov, *Applied Catalysis* A-*General*, **3**, 256 (2003).
11. Y. Song, H. Liu and D. He. *Energy Fuels*, **24**, 2817 (2010).
12. S. Wang, K. Murata, T. Hayakawa, S. Hamakawa and K. Suzuki, *Energy Fuels*, **15**, 384 (2001).
13. Y. P. Tong, L. Lu, X. J. Yang and X. Wang, *Solid State Science*, **1379**, 10 (2008).
14. H. F. Guo, P. Yan, X. Y. Hao and Z. Z.Wang, *Materials Chemistry and Physics*, **1065**, 112 (2008).
15. Z. C. Wang, H. F. Shui, Y. N. Zhu and J. S. Gao, *Fuel*, **885**, 88 (2009).
16. Z. Q. Ye, H. R. Chen, X. Z.Cui, J. Zhou and J. L. Shi, *Materials Letters*, **2303**, 63(2009).
17. C. L. Chen, X. K. Wang and M. Nagatsu, *Environmental Science and Technology*, **43**, 2362 (2009).
18. V. Alvin Shubert and Timothy S. Zwier, *The Journal of Physical Chemistr*y A, **111**, 13283 (2007).
19. J. R.Sohn and D. H. Seo, *Catalysis Today*, **219**, 87 (2003).
20. X. Lv, L. Wu, J. Wang, J. Li and Y. Qin, *Journal of Agricultural and Food Chemistry*, **59**, 256 (2011).
21. J. Liu, Y. Bin and M. Matsuo, *The Journal of Physical Chemistry* C, **116**, 134 (2012).
22. M. Mohapatra, D. Behera, S. Layek and S. Anand, *Crystal Growth and Design*, **12**, 18 (2012).
23. Y. Yanshen and L. Jia. *Zirconia Ceramics and its Composites*, (Beijing 2003)
24. J. K. Han, F. Saito and B. T. Lee, *Materials Letters*, **2181**, 58 (2004).
25. J. R. Sohn, S. H. Lee and J. S. Lim, *Catalysis Today* , **143**, 116 (2006).
26. J. Gass, P. Poddar, J. Almand, S. Srinath and H. Srikanth, *Advanced Functional Materials*, **71**, 16 (2006).
27. I. J. Bruce, J. Taylor, M. Todd, M. J.Davies, E. Borioni, C. Sangregorio and T. Sen, *Journal of magnetism and magnetic materials*, **145**, 284 (2004).
28. J. L. Ropero-Vega, A. Aldana-Pérez, R. Gómez, and M. E. Nino-Gómez. *Applied Catalysis* A*: General*, **379**, 24 (2010).